Physics and Imaging in Radiation Oncology 24 (2022) 1–6

Contents lists available at ScienceDirect

Physics and Imaging in Radiation Oncology

journal homepage: www.sciencedirect.com/journal/physics-and-imaging-in-radiation-oncology

First clinical experience with real-time portal imaging-based breath-hold monitoring in tangential breast radiotherapy

Elena N. Vasina [a,*], Natalie Kong [b], Peter Greer [a,b], Jose Baeza Ortega [a], Tomas Kron [c], Joanna J. Ludbrook [b], David Thwaites [d], Joerg Lehmann [a,b,d]

[a] School of Information and Physical Sciences, University of Newcastle, Newcastle, Australia
[b] Department of Radiation Oncology, Calvary Mater Newcastle, Newcastle, Australia
[c] Peter MacCallum Cancer Centre, Melbourne, Victoria, Australia
[d] Institute of Medical Physics, School of Physics, University of Sydney, Sydney, Australia

ARTICLE INFO

Keywords:
Real-time monitoring
Electronic portal imaging device
EPID
Tangential breast radiotherapy
Internal anatomy
Deep inspiration breath-hold
DIBH
Lung depth
Intra-fraction motion

ABSTRACT

Background and purpose: Real-time treatment monitoring with the electronic portal imaging device (EPID) can conceptually provide a more accurate assessment of the quality of deep inspiration breath-hold (DIBH) and patient movement during tangential breast radiotherapy (RT). A system was developed to measure two geometrical parameters, the lung depth (LD) and the irradiated width (named here skin distance, SD), along three user-selected lines in MV EPID images of breast tangents. The purpose of this study was to test the system during tangential breast RT with DIBH.

Materials and methods: Measurements of LDs and SDs were carried out in real time. DIBH was guided with a commercial system using a marker block. Results from 17 patients were assessed. Mean midline LDs, <mLDs>, per tangent were compared to the planned mLDs; differences between the largest and smallest observed <mLDs> (<mSDs>) per tangent were calculated.

Results: For 56% (162/288) of the tangents tested, <mLDs> were outside the tolerance window. All but one patient had at least one fraction showing this behaviour. The largest difference found between an <mLD> and its planned mLD was −16.9 mm. The accuracy of patient positioning and the quality of marker-block-based DIBH guidance contributed to the differences. Fractions with patient position verification using a single EPID image taken before treatment showed a lower rate (34%), suggesting reassessment of setup procedures.

Conclusions: Real-time treatment monitoring of the internal anatomy during DIBH delivery of tangential breast RT is feasible and useful. The new system requires no additional radiation for the patient.

1. Introduction

In tangential breast radiotherapy (RT) for curable breast cancer, treating under deep-inspiration breath-hold (DIBH) reduces the dose to the critical organs at risk: the heart, the lungs, and the liver. DIBH is now considered the standard of care for dose reduction to the heart and lung. Currently, the guidance of DIBH is often assessed via surrogates, e.g. a reflective marker block placed on the patient's abdomen [1], the volume of inhaled air [2], the skin surface [3,4], the radiation field lights or the treatment room lasers [5]. Depending on the patient's size and anatomy, the surrogate-based systems can make incorrect assessments of the position of the target and the organs at risk, potentially leading to significant deviations of the delivered dose from the planned dose [6].

Electronic portal imaging devices (EPIDs) can provide real-time images of the patient's irradiated anatomy during treatment. At present, they are generally only used for position verification before irradiation. Retrospective studies of MV images of tangential breast fields recorded with EPIDs in cine-mode showed that assessment of the quality of DIBH with external surrogates may lead to occasional significant errors [7]. Bossuyt et al. [8] detected positioning errors and incorrect breath-hold instances in tangential breast treatments by retrospective analysis of MV dose images using commercial EPID dosimetry software.

Geometrical parameters measured in the images of breast tangents such as the lung depth (LD), the irradiated width (named here the skin distance, SD), the craniocaudal distance (CCD), and the central heart distance (CHD) can help to estimate the positioning accuracy and the

* Corresponding author at: School of Information and Physical Sciences, University of Newcastle, University Drive, Callaghan, NSW 2308, Australia.
E-mail address: elena202@yahoo.com (E.N. Vasina).

https://doi.org/10.1016/j.phro.2022.08.002
Received 30 September 2021; Received in revised form 9 August 2022; Accepted 9 August 2022
Available online 13 August 2022

quality of DIBH [9,10]. The LD is the distance from the posterior radiation field edge to the chest wall, and the SD is the distance from the posterior radiation field edge to the skin surface of the breast (Fig. 1).

A system for measuring LDs and SDs during tangential breast cancer RT was developed and tested with RT phantoms [11–13]. It consists of software for acquiring single MV EPID frames in real time and an image processing application. This study reports on the first clinical, albeit observational, experience with the system.

2. Materials and methods

2.1. Ethics and patient selection

The study was approved by the Hunter New England Human Research Ethics Committee, Australia, 2020/ETH00720, and conducted at the Calvary Mater Newcastle hospital. The patients consented to participate. Data from 17 patients who received tangential breast RT with DIBH with our clinical Real-time Position Management™ system (RPM, Varian Medical Systems, Palo Alto, CA), and who were monitored for at least three fractions were included in this study. Five of the 17 patients (nos. 3, 5, 6, 12, 16) were treated for right-sided breast cancer.

2.2. Treatment simulation and planning

The patients were simulated on a Siemens Somatom CT scanner (Siemens Medical Systems, Erlangen, Germany) in the supine position with a knee-fix, inclined on a breast board (MT-250, MedTech, Orange City, IA) with the arms elevated. Skin tattoos were applied to support positioning. DIBH was guided by the RPM system. Prior to simulation, the patients demonstrated the ability to hold their breath for 20 s consecutively for at least 4 breath-holds. The Eclipse treatment planning system (Varian Medical Systems, Palo Alto, CA) was used to create the tangential plans. Two tangential photon beams of 6 MV or four beams of 6 MV and 10, 15 or 18 MV were employed to deliver a dose of 40 Gy in 15 fractions to the breast. Some of the beams contained about 20% forward planned step and shoot modulation towards the end. Patient 2 had three beams: 6 and 15 MV for the first tangent and 6 MV for the second.

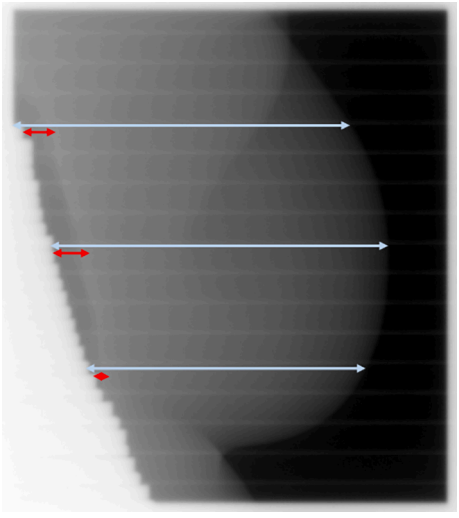

Fig. 1. MV EPID image of a tangential breast field illustrating the lung depth (LD) in red and the skin distance (SD) in light blue. Both parameters are shown at the default locations (superior, midline, and inferior at 25%, 50% and 75% of the field height, respectively). These locations are user selectable and should be chosen to be clinically optimal based on the anatomy. (For interpretation of the references to colour in this figure legend, the reader is referred to the web version of this article.)

2.3. Patient setup and DIBH monitoring during treatment

The patients were positioned using the skin tattoos and aligned to the room laser system. As per local procedure for all breast patients, single EPID images of the first medial treatment beam were collected in breath-hold during the first three fractions. Based on the images, position correction was done once, at fraction 4, and carried through the rest of the treatment. If clinically required, additional EPID images prior to treatment with immediate position correction were taken past fraction 4. Breath-holds were monitored using the RPM with a breath-hold tolerance window (TW) of 5 mm. The RPM marker block was placed on the midline lower sternum (or upper abdomen for large patients).

2.4. Real-time LD and SD measurements

The new system to assess LD and SD in real time [13] relies on a custom connection to the linac's imaging system via a frame grabber card. It comprises two components: an application for acquiring single MV EPID frames in TIFF format in real time, C-DOG [14], and an image processing application, LEILA (Live EPID-based Inspiration Level Assessment). The workflow of the system is shown in Fig. 2. LEILA is coded in C#. It analyses row profiles of the MV frames and measures LDs and SDs at three user-specified locations. The system allows for measurements in images of open tangential breast fields and fields partially blocked by the multi-leaf collimator (MLC). The algorithm was developed using over 1,000 MV EPID images of breast tangents and tested with phantoms [11–13]. The tests demonstrated sub-millimetre relative accuracy, and a latency <350 ms. Differences in patient anatomy and imaging systems add an uncertainty of 2 mm to LD and SD measurements in patients, as estimated from the data.

The algorithm measures the radiation field length and compares it with its planned value. The latter is input via the DICOM plan file before treatment commences and stored by the application. If the radiation field length partially extends beyond the EPID (either the top or bottom boundary), the algorithm will calculate the location of the user-defined lines taking into account the missing part of the field. The user interface presents measured LDs at the three lines of interest both in graphical form and as numerical values. The LD and SD values, the corresponding timestamps and the filenames of the TIFF files are saved in a text file.

The system was used in parallel to the standard clinical procedures and in accordance with the ethics approval. It was not intended to alter the clinical workflow or clinical decisions. The system was employed to monitor clinical treatment accuracy and to provide data for later approval for routine clinical use. The RPM automatically triggered beam-on when its assessment of the patient's breath-hold level was within the 5 mm TW. During dose delivery, LD and SD parameters were measured at the three default locations (Fig. 1). Measured midline LDs were graphically compared to the planned values. Separate in-house software assisted in determining the planned values in DRR images of the treatment fields. This software displays the image row profiles to simplify manual measurements of LDs and SDs and reduce errors due to visual bias; the intra-user variation is below 1 mm.

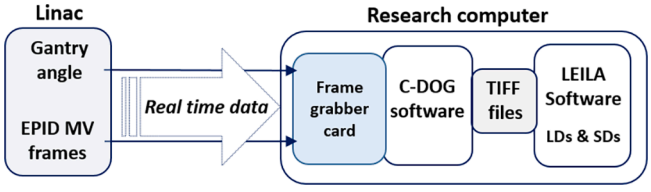

Fig. 2. Workflow of real-time recording of MV frames with the C-DOG software and real-time measurements of LD (lung depth) and SD (skin distance) with the image processing software.

2.5. Data analysis

For Patient 1, the LDs and SDs measured at the three default locations were compared to the planned values. For all patients mean midline LDs, <mLDs>, mean across the fraction duration, were calculated per tangent and compared with the planned midline LDs. For the tests, the RPM TW of 5 mm was translated into a 6 mm TW. This takes into account the geometric relationship between the RPM TW and its projection on the EPID (which results in approx. 4 mm and depends on the tangent) and adds 2 mm to account for patient and EPID specific uncertainty as per section 2.4.

To allow for retrospective assessment of treatment consistency while avoiding possible uncertainties in the planned values, differences between the largest and smallest observed mean midline LDs (SDs) per tangent were calculated. They are defined by

$$< \mathrm{mLD} >_{\mathrm{range}} = < \mathrm{mLDs} >_{\mathrm{max}} - \ < \mathrm{mLDs} >_{\mathrm{min}}.$$

and

$$< \mathrm{mSD} >_{\mathrm{range}} = < \mathrm{mSDs} >_{\mathrm{max}} - \ < \mathrm{mSDs} >_{\mathrm{min}},$$

where $<\mathrm{mLDs}>_{\mathrm{max}}$ and $<\mathrm{mLDs}>_{\mathrm{min}}$ are the maximum and minimum values of <mLDs> observed per patient per tangent, and $<\mathrm{mSDs}>_{\mathrm{max}}$ and $<\mathrm{mSDs}>_{\mathrm{min}}$ are the maximum and minimum values of <mSDs> observed per patient per tangent.

3. Results

3.1. Intra-beam and intra-fraction variations

For all patients the intra-beam changes of midline LDs and SDs were within 3 mm when the beams were delivered in a single breath-hold. These changes could reach 5 mm when multiple breath-holds were required to deliver one beam, and for other beams delivered at the same tangent (with a different breath-hold). This is illustrated for a representative fraction of Patient 1 in Fig. 3, which shows the time-resolved behaviour of the LDs and SDs.

3.2. Inter-fraction variations

Only for one of the patients were the measured <mLDs> within the TW during all observed fractions (Table 1). For every other patient, the <mLDs> were outside the 6 mm TW for at least one fraction. The maximum difference between <mLDs> and the planned mLDs found was −16.9 mm. Overall, for 56% (162/288) of tangents tested, the <mLDs> were outside the TW. For the first tangent treated, 63% (85/136) of all fractions were outside the TW. For those fractions where a single EPID image (sEPID) was used for position verification, 34% (14/41) were outside the TW. For the second tangent, 51% (77/152) of all fractions were outside the TW. Here, 33% (18/55) of the fractions with sEPID were outside the TW. For the five patients who did not clinically require any additional EPID images prior to treatment after the initial three fractions and correction at the fourth, 73% (27/37) and 57% (21/37) of fractions were outside the TW for the first and second tangents, respectively.

The mean differences between the measured LDs and SDs and their

Table 1
Per tangent mean midline lung depth (<mLD>) assessment for all patients: relation to tolerance window (TW), maximum deviation from the planned midline LD and number of fractions of <mLD> outside TW in total and for fractions with single EPID position verification prior to treatment (sEPID).

Patient	<mLD> vs TW	Maximum of [<mLD> – planned mLD], mm	Number of fractions with <mLD> outside TW/Total number of fractions		Number of fractions with sEPID outside TW/Number of fractions with sEPID	
			Gantry angle 1*	Gantry angle 2	Gantry angle 1*	Gantry angle 2
1	Below & Above	−16.2	11/14	10/14	1/2	0/2
2	Below	−6.8	7/10	4/12	7/10 [KV]	4/12
3	Below & Above	10	5/9	4/10	0/1	2/2
4	Below	−9.5	9/14	8/14	2/5	0/5
5	Below	−10.3	9/10	9/10	0/1	0/1
6	Above	10.5	9/10	5/14	NA	0/4
7	Below	−13.3	8/8	7/8		
8	Below	−7.9	9/11	6/11		
9	Below	−10.7	3/8	8/8	2/7	7/8
10	Below & Above	−6.2	1/3	4/5	1/1	3/2
11	Within	−2.3	0/12	0/12	0/12	0/12
12	Below	−8.1	3/3	3/3		
13	Below	−7.1	5/12	4/12		
14	Below	−3.4	1/6	2/8	NA	1/2
15	Above	8.6	2/3	1/3		
16	Above	3.4	NA	1/3	NA	1/3
17	Below	−8.4	3/3	1/5	1/2	0/2

*Due to clinical imaging for position verification, some of the first beams were not available for observation for patients 1, 2, 3, 6, 10, 14, 16, and 17. NA: not available.

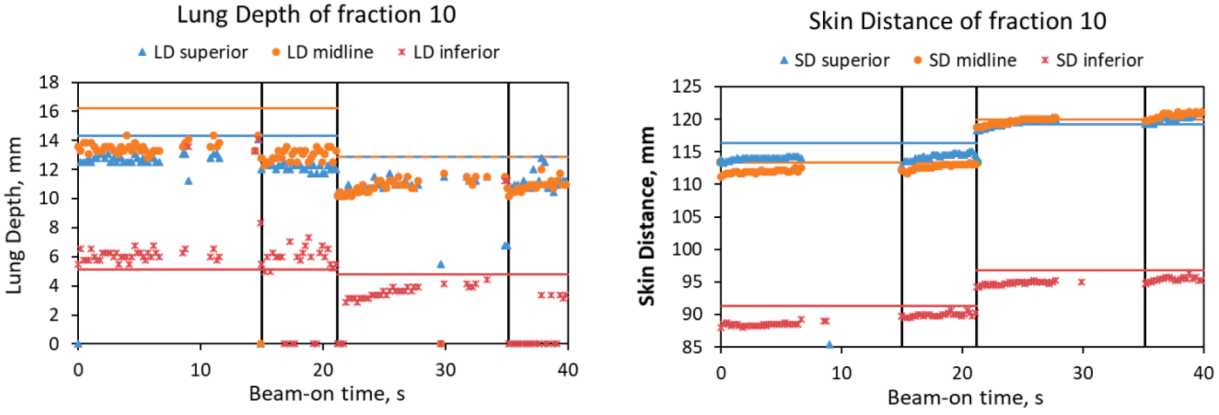

Fig. 3. Lung depth (LD) and skin distance (SD) vs beam-on time during fraction 10 of Patient 1. Vertical lines separate the four beams. LDs and SDs are close to their planned values (shown by the horizontal lines of the same colour). Short beam-off instances are present in the second halves of beams 1 and 3 when the MLC leaves come in: this is seen as the gaps between the data points of LDs (beam-holds). When the MLC leaves block the patient's skin, the measured SDs become 0 mm (data not shown).

planned values for every treatment fraction of Patient 1 (Fig. 4) illustrate notable differences between the fractions. Due to instances of position verification via sEPID, some of the first beams were not available for the tests. Differences > 6 mm were observed between the planned and measured LDs and SDs for 11 of 14 fractions. The maximum range of the differences was about 20 mm for beam 3 between fractions 5 and 6, going in opposite directions.

The maximum $<mLD>_{range}$ and $<mSD>_{range}$ observed was 20.5 and 20.4 mm, respectively (Table 2). Most of the patients with naturally large tissue width, mSD-mLD => 60 mm, (Patients 1, 4, 5, 7, 9, 10, 11, 15, and 16), not including a patient with a tissue expander (Patient 2), showed larger range values. No differences were observed between the left- and right-sided breast treatments.

Table 2
Ranges of the mean midline LDs and SDs: Difference between largest and smallest mean (per tangent) measured throughout the treatment.

Patient	Gantry angle 1		Gantry angle 2	
	$<mLD>_{range}$ [mm]	$<mSD>_{range}$ [mm]	$<mLD>_{range}$ [mm]	$<mSD>_{range}$ [mm]
1	20.5*	18.1	18.7*	20.4
2	4.7	3.9	3.0	3.3
3	12.5	10	10	8.5
4	11.8*	14.2	10.5*	17.2
5	8.4	10.3	8.7	10.2
6	7.7	8.5	9.9	9.7
7	8.3	6.8	11.8*	8.4
8	5.3	5.3	5.5	5.6
9	6.6	7.9	4.7	6.2
10	5.9	7.6	10	8.4
11	2.7	6.6	3.1	10.8
12	2.4	2.3	3.4	3.8
13	5.1	3.9	8.9	7.4
14	6	5	5	5.5
15	6.1	5	3.1	5.3
16	NA	NA	6.4	8.1
17	4.8	bolus	9.5	bolus

*The asterisks indicate that values can be underestimated due to instances of midline LDs being recorded as 0 mm and hence possibly being negative (chest wall not fully in the beam). NA: not available.

4. Discussion

A new software system assessing the patient position using imaged internal anatomy during breath-hold was tested as an observational tool for patients undergoing tangential breast cancer RT with DIBH. The DIBH was controlled following the standard local protocol using the RPM method. The system measured LDs and SDs in portal MV images of the breast tangents in real time during treatment delivery.

Differences between the mean midline LD of a treatment fraction and the corresponding planned midline LD were found to be larger than the TW for more than half of the tangents tested. For ten and three of the 17 patients the <mLDs> were always below or above the TW, respectively (Table 1). Three patients showed <mLDs> both above and below the TW. For one patient all <mLDs> were inside the TW. These observations confirmed the results of earlier work [6] that for at least part of the treatment the guidance with RPM alone was suboptimal. Assessments of the ranges of the mean midline LDs and SDs, which remove uncertainties associated with the planned values and reduce patient specific uncertainties of the image processing software, supported these finding. The accuracy of the patient setup and the quality of DIBH guidance both contributed to the differences between the measured and planned parameters. The inter-fraction differences observed in this study suggested that deviations in the setup were the dominant factor, as changes of LD and SD within one fraction were smaller. A new surface-guided system for patient setup is currently being implemented in the department.

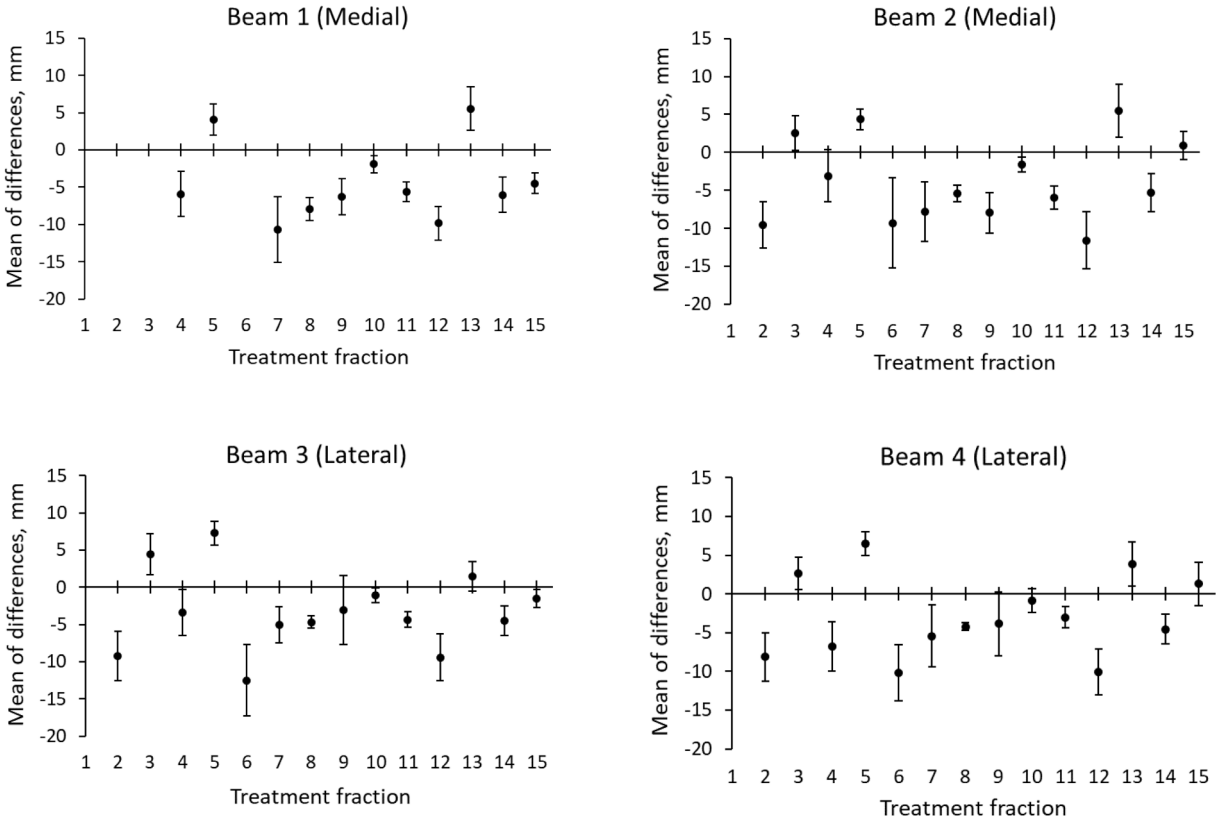

Fig. 4. The differences between the measured and the planned LD and SD values (superior, midline, and inferior parameters are grouped together) for each beam of the tangential breast treatment of Patient 1. Plotted are the mean values with the error bars representing one standard deviation. The planned LDs and SDs are provided in Supplementary Table 1S.

The intra-beam changes of LDs and SDs were similar to the results reported by Jensen et al. [15]. They measured the position of the chest wall's edge in retrospective cine EPID images of breast cancer patients treated with DIBH and evaluated the performance of two non-commercial surface-guided RT techniques. The authors found that intra-beam variations of the chest wall's edge were <3 mm.

For multiple breath-hold instances during one beam, changes in LDs and SDs of up to 5 mm were observed [16]. This suggests that when the patient left the breath-hold position, the RPM system was able to detect the corresponding excursions of the chest (or abdomen). The RPM triggered the beam off when the recorded position was outside its TW, and back on when the position was again inside the TW, resulting in the LDs and SDs remaining within 5 mm. However, comparably larger patient setup errors went undetected by the RPM, as seen by the differences from the planned values. This can be partially explained by possibly inconsistent positioning of the RPM block and by "re-baselining" of the RPM system, which is performed regularly in clinical practice if the patient is unable to reach the breath-hold window. The limited use of position verification with MV port films as described above possibly contributes to this.

Rong et al [4] measured the chest wall excursions in retrospective MV cine images of breast tangents taken at the mid-point of the beam-on time. The study investigated the target position, the accuracy and reproducibility of the RPM and AlignRT (Vision RT Ltd, London, UK) systems. The authors found an inferior correlation between the RPM and the target position during DIBH. They concluded that the target position accuracy could be improved by AlignRT in addition to RPM. Penninkhof et al. [17] evaluated three clinical DIBH techniques for breast cancer RT: from portal imaging during treatment to continuous monitoring with the AlignRT system. The authors found that a daily imaging and online setup correction were required for accurate treatment delivery. A more accurate image registration (via cone-beam CT) was observed when patients were positioned with AlignRT.

Poulsen et al. [18] designed an algorithm based on changes in pixel intensity due to the heartbeat to automatically detect the heart edge in MV cine images of breast tangents. The retrospective study demonstrated the high efficiency of the algorithm for heart exposure detection. The real-time clinical application of this method has not yet been reported.

This study showed the technical feasibility and robustness of the new system. It identified a number of small implementation issues, which had not been seen during tests with RT phantoms [13], and for which the software was modified. These included analysis to skip empty frames produced during beam-hold when the patient is outside the TW, as assessed by RPM, and no radiation is delivered. Additionally, a filter based on standard deviation was devised to skip empty frames containing afterglow images of the previous frames, and also partial frames which occur due to incomplete beam-on or beam-off instances. And finally, code was added to take into account the loss of signal related to horizontal bands (lines) occurring in images of single MV frames due to signal readout.

As the system uses separate software tools for image acquisition and image processing, it can be easily adapted to using another image acquisition software, for instance with another linac vendor. Such software would need to provide the image matrix, the gantry angle (tangent), the collimator angle in the filenames or with the image matrix, and the pixel size of the EPID.

Currently, three LDs and three SDs are reported by the system; future work will study how to convert these parameters into one allowing for more streamlined feedback to the treatment staff and direct guidance to the patient. This will take into account that not all parameters can be assessed for all images throughout the treatment, due to partial blocking of the field by MLC leaves, especially when more modulated fields are used. In this context, SD was shown to be more reliable to measure, as the skin–air interface can be detected with higher certainty and less variation [13]. However, SD is likely affected by inter-fractional changes to the anatomy, like swelling of the breast. Hence differentiation between those and intra-fractional changes will need to be made. The number of the geometrical parameters measured can be increased with minimal cost in terms of processing time. Factors that can affect the accuracy of measurements are MLC positioning errors, afterglow in the EPID images, and large clusters of "dead" pixels of EPIDs.

The image processing software can be employed offline to visualize trends in chest wall motion along its whole length. Such data will present a source of data mining for quality improvement similar to that of surface-guided RT data [19]. The system can also be applied during free breathing tangential breast treatments and help to monitor the patient's motion due to muscle relaxation [20,21]. For the system to be used as a sole DIBH monitoring tool, logistics in terms of the workflow will need to be addressed since information is only available during dose delivery. Because of the near-universal availability of EPID panels on linacs, this system offers an attractive alternative to other DIBH monitoring systems while inherently being more accurate. Using practical action thresholds the treatment can be interrupted when required, thus avoiding large deviations, like those reported in this study.

In conclusion, this study presented the first clinical tests of the Live EPID-based Inspiration Level Assessment (LEILA) software for real-time measurements of LDs and SDs during tangential breast RT. It demonstrated that the magnitude of inter-fraction variabilities of LD and SD were higher than expected based on the external surrogate-based monitoring with RPM. The new system will increase patient safety by improving the accuracy of treatment delivery and help achieve the sparing of the organs at risk and target coverage as per the treatment plan. It employs imaging hardware available on most treatment machines and it gives no additional radiation to the patient.

Declaration of Competing Interest

The authors declare that they have no known competing financial interests or personal relationships that could have appeared to influence the work reported in this paper.

Acknowledgements

The authors thank the patients for their participation in the study and the radiation therapists of the CMN hospital for their assistance. They thank Dr S. Bhatia, the initial developer of C-DOG software. This work was supported by National Health and Medical Research Council (NHMRC) grant 1147533 of the Australian Government. The contents of the published material are solely the responsibility of the authors and do not reflect the views of NHMRC.

Appendix A. Supplementary data

Supplementary data to this article can be found online at https://doi.org/10.1016/j.phro.2022.08.002.

References

[1] Pandeli C, Smyth LML, David S, See AW. Dose reduction to organs at risk with deep-inspiration breath-hold during right breast radiotherapy: a treatment planning study. Radiat Oncol 2019;14:1–10. https://doi.org/10.1186/s13014-019-1430-x.

[2] Mittauer KE, Deraniyagala R, Li JG, Lu B, Liu C, Samant SS, et al. Monitoring ABC-assisted deep inspiration breath hold for left-sided breast radiotherapy with an optical tracking system. Med Phys 2015;42:134–43. https://doi.org/10.1118/1.4903511.

[3] Kalet AM, Cao N, Smith WP, Young L, Wootton L, Stewart RD, et al. Accuracy and stability of deep inspiration breath hold in gated breast radiotherapy - A comparison of two tracking and guidance systems. Phys Med 2019;60:174–81. https://doi.org/10.1016/j.ejmp.2019.03.025.

[4] Rong Y, Walston S, Welliver MX, Chakravarti A, Quick AM. Improving intra-fractional target position accuracy using a 3D surface surrogate for left breast irradiation using the respiratory-gated deep-inspiration breath-hold technique. PLoS ONE 2014;9:e97933.

[5] Bartlett FR, Colgan RM, Donovan EM, Carr K, Landeg S, Clements N, et al. Voluntary breath-hold technique for reducing heart dose in left breast radiotherapy. J Vis Exp 2014;89:e51578.
[6] Doebrich M, Downie J, Lehmann J. Continuous breath-hold assessment during breast radiotherapy using portal imaging. Phys Imaging Radiat Oncol 2018;5:64–8. https://doi.org/10.1016/j.phro.2018.02.006.
[7] Lutz CM, Poulsen PR, Fledelius W, Offersen BV, Thomsen MS. Setup error and motion during deep inspiration breath-hold breast radiotherapy measured with continuous portal imaging. Acta Oncol 2016;55:193–200. https://doi.org/10.3109/0284186X.2015.1045625.
[8] Bossuyt E, Weytjens R, Nevens D, De Vos S, Verellen D. Evaluation of automated pre-treatment and transit in-vivo dosimetry in radiotherapy using empirically determined parameters. Phys Imaging Radiat Oncol 2020;16:113–29. https://doi.org/10.1016/j.phro.2020.09.011.
[9] Fein DA, McGee KP, Schultheiss TE, Fowble BL, Hanks GE. Intra- and interfractional reproducibility of tangential breast fields: A prospective on-line portal imaging study. Int J Radiat Oncol Biol Phys 1996;34:733–40. https://doi.org/10.1016/0360-3016(95)02037-3.
[10] Michalski A, Atyeo J, Cox J, Rinks M. Inter- and intra-fraction motion during radiation therapy to the whole breast in the supine position: A systematic review. J Med Imag Radiat Oncol 2012;56:499–509. https://doi.org/10.1111/j.1754-9485.2012.02434.x.
[11] Vasina E, Greer P, Lehmann J. Verification of new software for assessment of the quality of deep inspiration breath hold (DIBH) in radiotherapy of breast cancer. Real-time measurements of the lung depth with radiotherapy phantoms [abstract]. Asia-Pac J Clin Oncol 2020;16:42–3. https://doi.org/10.1111/ajco.13473.
[12] Vasina E, Greer P, Thwaites D, Lehmann J. Verification of a system for real-time EPID based breath hold monitoring during DIBH tangential breast cancer radiotherapy [abstract]. Med Phys 2021;48:111. https://doi.org/10.1002/mp.15041.
[13] Vasina EN, Greer P, Thwaites D, Kron T, Lehmann J. A system for real-time monitoring of breath-hold via assessment of internal anatomy in tangential breast radiotherapy. J Appl Clin Med Phys 2022;23:1–15. https://doi.org/10.1002/acm2.13473.
[14] Nguyen DT, O'Brien R, Kim JH, Huang CY, Wilton L, Greer P, et al. The first clinical implementation of a real-time six degree of freedom target tracking system during radiation therapy based on Kilovoltage Intrafraction Monitoring (KIM). Radiother Oncol 2017;123:37–42. https://doi.org/10.1016/j.radonc.2017.02.013.
[15] Jensen C, Urribarri J, Cail D, Rottmann J, Mishra P, Lingos T, et al. Cine EPID evaluation of two non-commercial techniques for DIBH. Med Phys 2014;41:021730. https://doi.org/10.1118/1.4862835.
[16] Vasina E, Kong N, Greer P, Govindarajulu G, Ludbrook J, Lehmann J. Monitoring DIBH via measurements of the lung depth during tangential breast cancer radiotherapy [abstract]. Asia-Pac J Clin Oncol 2021;17:15–6. https://doi.org/10.1111/ajco.13682.
[17] Penninkhof J, Fremeijer K, Offereins-van Harten K, van Wanrooij C, Quint S, Kunnen B, et al. Evaluation of image-guided and surface-guided radiotherapy for breast cancer patients treated in deep inspiration breath-hold: A single institution experience. Tech Innov Patient Support Radiat Oncol 2022;21:51–7. https://doi.org/10.1016/j.tipsro.2022.02.001.
[18] Poulsen PR, Thomsen MS, Hansen R, Worm E, Spejlborg H, Offersen B. Fully automated detection of heart irradiation in cine MV images acquired during breast cancer radiotherapy. Radiother Oncol 2020;152:189–95. https://doi.org/10.1016/j.radonc.2019.11.006.
[19] Jacqmin D. Surface-guided radiotherapy systems as source of big data: using Sgrt data to study the radiotherapy process [abstract]. Int J Radiat Oncol Biol Phys 2019;105:E731–2. https://doi.org/10.1016/j.ijrobp.2019.06.823.
[20] Kinoshita R, Shimizu S, Taguchi H, Katoh N, Fujino M, Onimaru R, et al. Three-dimensional intrafractional motion of breast during tangential breast irradiation monitored with high-sampling frequency using a real-time tumor-tracking radiotherapy system. Int J Radiat Oncol Biol Phys 2008;70:931–4. https://doi.org/10.1016/j.ijrobp.2007.10.003.
[21] Jensen CA, Roa AMA, Lund JA, Frengen J. Intrafractional baseline drift during free breathing breast cancer radiation therapy. Acta Oncol 2017;56:867–73. https://doi.org/10.1080/0284186X.2017.1288924.